

$V^{III}V^{IV}(HPO_4)_4 \cdot nH \cdot H_2O$: a mixed-valence vanadium phosphate with an open framework

Nathalie Calin,^a Christian Serre^b and Slavi C. Sevov^{*a}

^aDepartment of Chemistry and Biochemistry, University of Notre Dame, Notre Dame, IN 46556, USA

^bInstitut Lavoisier, Université de Versailles-St. Quentin en Yvelines, UMR CNRS 8637, 45 Avenue des Etats-Unis, 78035 Versailles cedex, France

Received 12th August 2002, Accepted 19th December 2002

First published as an Advance Article on the web 16th January 2003

The title compound was hydrothermally synthesized from elemental vanadium, phosphoric and boric acids, and ethylenediamine. It is isostructural with the mixed-valence titanium phosphate $Ti^{III}Ti^{IV}(HPO_4)_4 \cdot nH \cdot H_2O$ (TPO-2) but differs in electronic states and in its magnetic properties. The structure [tetragonal, $I4_1$, $a = 6.3881(4)$ and $c = 16.608(1)$ Å] is of the open-framework type and is composed of corner-sharing VO_6 octahedra and $PO_3(OH)$ tetrahedra. This creates eight-membered rings in which water molecules and organic moieties alternate with terminal hydroxyl groups. IR, TGA, and magnetic measurements confirm the structure and the oxidation states of vanadium. The compound loses the template and water molecules above 380 °C, but preserves its structure in the form of vanadium(IV) phosphate $[V^{IV}(HPO_4)_2]$, $I4_1$, $a = 6.374(1)$ and $c = 16.360(4)$ Å]. Thermogravimetry shows that the structure collapses above 450 °C. The presence of reduced vanadium provides potential for redox catalytic properties.

1 Introduction

Organically templated transition metal phosphates show diverse structural chemistry; in particular, structures of the open-framework type are interesting as potential redox catalysts, especially when the transition metal is reduced or of mixed valence.^{1–3} The hydrothermal approach is usually the method of choice for such syntheses, and organic mono- and polyamines are the most commonly used templates. A convenient way to achieve open-framework compounds containing reduced or mixed-valence transition metals is to use the metal in its elemental form in the reaction mixture. Often, this turns out to be the only method for the synthesis of compounds with reduced or mixed-valence transition metals. For titanium, this approach has led to the diaminopropane (dap)- and ethylenediamine (en)-templated materials $Ti^{III}Ti^{IV}(PO_4)(HPO_4)_2 \cdot (H_2O)_2 \cdot (dapH_2)_{0.5}$ (TPO-1) and $Ti^{III}Ti^{IV}(HPO_4)_4 \cdot nH \cdot H_2O$ (TPO-2), respectively.^{4,5} Similarly, using elemental iron results in the mixed-valence iron arsenate $Fe^{III}Fe^{II}F_2(HAsO_4)(AsO_4) \cdot nH_2 \cdot 2H_2O$, while molybdenum produces the novel Dawson-like molybdenum borophosphate anion $[Mo^V_5Mo^{VI}_7O_{22}(BO_4)_2(PO_4)_5(HPO_4)_3]^{8-}$.^{6,7} Here we report on the outcome of the same approach applied to vanadium: a new mixed-valence V^{III}/V^{IV} phosphate with an open-framework structure, $V^{III}V^{IV}(HPO_4)_4 \cdot nH \cdot H_2O$ (**1**), and the product of its calcination at 400 °C, $V^{IV}(HPO_4)_2$ (**2**). Only a few other mixed-valence V^{III}/V^{IV} compounds with open frameworks are known.^{8–15}

2 Experimental

Synthesis

The title compound was synthesized hydrothermally from a reaction mixture designed to search for organically-templated mixed-valence vanadium borophosphates with open-framework structures analogous to known compounds with other transition metals. Thus, elemental vanadium (–325 mesh, 99.5%, Acros), phosphoric acid (85%, Fisher), boric acid (Acros), ethylenediamine (p. a., Acros), and distilled water were mixed in a molar ratio of 4:30:13:8:600, respectively

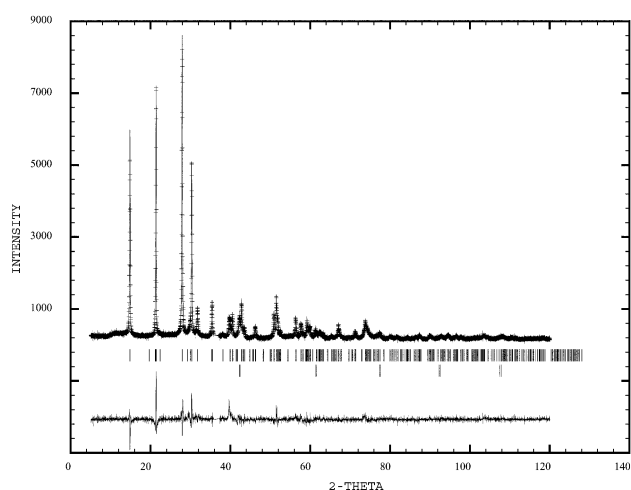
(pH < 2). The mixture was loaded into a Teflon-lined stainless steel autoclave with a capacity of 23 mL and was heated at 180 °C for 5 days. The solid product, a mixture of dark green powder and unreacted vanadium, was filtered out, washed, and dried. Although boron is not present in the product, all attempts to synthesize the compound without boric acid were unsuccessful. The synthesis was later optimized, and a single-phase product was obtained from a mixture of elemental vanadium, fluorophosphoric acid (70%, Acros), phosphoric acid, boric acid, ethylenediamine, and distilled water in a molar ratio of 2:30:30:13:16:1200, respectively. All attempts to grow single crystals suitable for structure determination by changing reaction temperature, concentrations, molar ratios, etc., were unsuccessful.

Structure determination

Powder X-ray diffraction data for the as-synthesized and calcined compounds were collected on a Bruker D8 diffractometer (Cu-K α , 2θ step = 0.02°, 60 s per step). The patterns were indexed based on the isostructural compound $Ti^{III}Ti^{IV}(HPO_4)_4 \cdot nH \cdot H_2O$ [$I4_1$; (**1**) $a = 6.3881(4)$ and $c = 16.608(1)$ Å; (**2**) $a = 6.374(1)$ and $c = 16.360(4)$ Å]. The structure of **1** was refined using Fullprof2001¹⁶ and WinPLOTR¹⁷ in the angular 2θ range 5–120° using 262 F_{obs} and a total of 43 variable parameters (a small 2θ region at 35.8–37.10° was excluded due to a small broad peak of unknown nature, and a second phase of unreacted vanadium metal was refined as well). Soft constraints were applied for the V–O and P–O interatomic distances. The phosphorus atoms were too close to their symmetry-generated equivalent positions and were, therefore, refined as half-occupied. The corresponding terminal oxygens bonded to the phosphorus atoms, i.e. the OH groups, and the ethylenediamine and water molecules were also refined as half-occupied. The latter two and the phosphate groups alternate in the structure. Details are given in Table 1 and the final Rietveld plot is shown in Fig. 1. The final agreement factors are: $R_p = 8.38\%$, $R_{wp} = 11.0\%$, and $R_{Bragg} = 10.8\%$. Positional parameters and essential distances are listed in Tables 2 and 3, respectively.

Table 1 Crystallographic data for **1**

M/g mol ⁻¹	564.8
Crystal system	Tetragonal (body centered)
Space group	<i>I</i> ₄ (no. 80)
<i>a</i> /Å	6.3881(4)
<i>c</i> /Å	16.608(1)
<i>V</i> /Å ³	677.73(8)
<i>Z</i>	2
Temperature/K	293
λ (Cu-K α_1 /K α_2)/Å	1.54059/1.54439
2θ Ranges/°	5–120.0
Step time/s	60
2θ Step size/°	0.02
Excluded area (2θ)/°	35.8–37.1
Total no. of reflections	262
Total no. points	5751
No. parameters	43
No. atoms refined	12
No. distance constraints	15
<i>R</i> _p (%)	8.38
<i>R</i> _{wp} (%)	11.0
<i>R</i> _{Bragg} (%)	10.8

**Fig. 1** Final Rietveld and difference plots for **1**.**Table 2** Atomic coordinates and occupancy factors for **1**

Atom	<i>x</i>	<i>y</i>	<i>z</i>	Occupancy (%)
V	0	0.5	0.1554(8)	100
P1	0.493(1)	−0.417(1)	0.1993(5)	50
P2	0.077(1)	0.004(2)	0.1096(5)	50
O1	0.685(2)	0.519(2)	0.152(1)	100
O2	0	0.5	0.2750(6)	100
O3	−0.011(3)	0.177(1)	0.159(1)	100
O4	0	0.5	0.0338(6)	100
O5	0.534(5)	0.170(2)	0.216(3)	50
O6	0.321(2)	0.005(9)	0.093(3)	50
Ow	0.5	0	0.239(1)	50
C	0.552(7)	−0.101(4)	0.1767(7)	50
N	0.551(5)	−0.135(3)	0.0810(7)	50

Properties

The magnetizations of 24 mg of **1** and 23 mg of **2** were measured on a Quantum Design MPMS SQUID magnetometer at a field of 3 T in the temperature range 10–250 K. Thermogravimetric analyses (TGA) were carried out on a CAHN TG-131 instrument both in air and nitrogen flows (80 mL min⁻¹), using a heating rate of 5 °C min⁻¹ up to 800 °C. X-Ray thermodiffractometry was performed under air with a D5000 Siemens diffractometer equipped with a high temperature stage (θ – θ mode, Co-K α λ = 1.7903 Å, temperature range

Table 3 Important distances (Å) in the structure of **1**

V–O1	2.02(1) × 2
V–O2	1.99(1)
V–O3	2.06(1) × 2
V–O4	2.02(1)
P1–O1	1.51(1)
P1–O1	1.52(1)
P1–O4	1.50(1)
P1–O5	1.61(1)
P2–O2	1.49(1)
P2–O3	1.49(2)
P2–O3	1.48(1)
P2–O6	1.58(1)

30–800 °C). IR spectra were collected using a Perkin-Elmer PARAGON-100 spectrometer in the region 400–4000 cm⁻¹ from pellets pressed with KBr.

3 Results

V^{III}V^{IV}(HPO₄)₄·*n*H₂O (**1**) is isostructural with Ti^{III}Ti^{IV}·(HPO₄)₄·*n*H₂O (TPO-2),⁵ a framework built from corner-sharing MO₆ octahedra and PO₃(OH) tetrahedra (Fig. 2 and 3). Crystallographically, there is only one metal and two phosphorus sites. The framework has open eight-membered rings that are occupied by the ethylenediamine (in *syn* conformation) and water molecules. Fig. 2 gives the impression that there are empty and occupied channels that alternate along *a*. This, however, is misleading because, in reality, the rings that “form” the channels are statistically occupied and empty along the *b* axis (the viewing direction in Fig. 2), or otherwise a superstructure would have been observed. This prevents the structure from becoming microporous after removal of the template because the process creates localized cavities rather than extended channels. The differences between the vanadium and titanium compounds are only in the lattice parameters and, subsequently, the metal–oxygen distances. Thus, the volume of

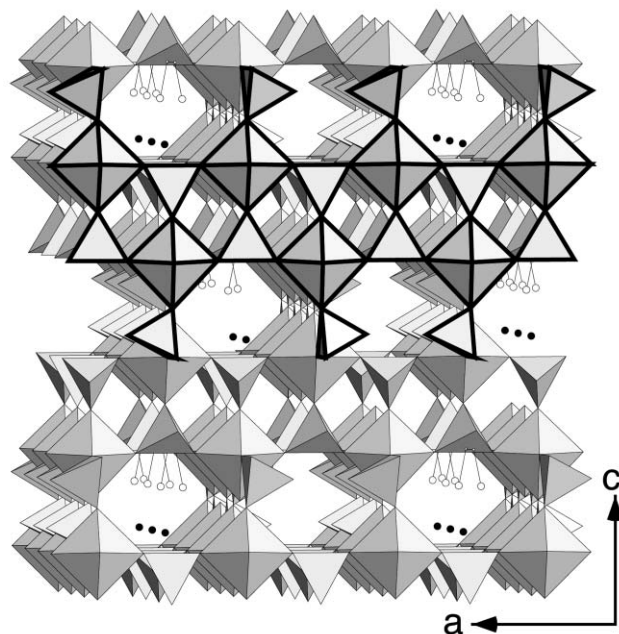


Fig. 2 Polyhedral view along *b* of the structure of the body-centered tetragonal (*I*₄) structure of **1**, where the tetrahedra and octahedra are centered on P and V, respectively. The terminal vertices of the tetrahedra are the OH groups. The ethylenediamine and water molecules (isolated filled circles) are shown as well. The framework part is identical to that of the calcined phase, V^{IV}V^{IV}(HPO₄)₄. The repeating building unit, a “double” chain along both the *a* and *b* axes, is outlined with thicker polyhedral edges.

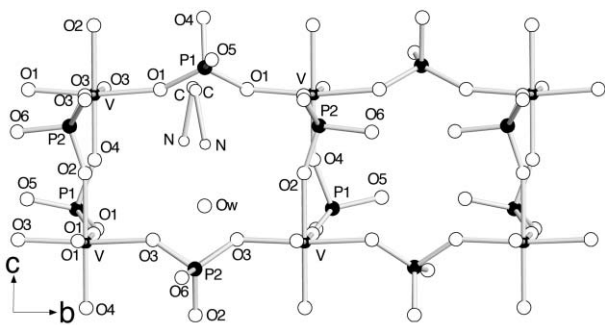


Fig. 3 A closer view of the structure of **1** (with the atoms labeled), showing two crystallographically equivalent rings. Due to the disorder of the phosphorus and O5 and O6 positions, the rings can be differently occupied (see text). The left ring is shown as occupied by the ethylenediamine and water molecules, and the right one has the hydroxyl groups of the four HPO_4 groups pointing inwards.

the vanadium compound, 677.7 \AA^3 , and the V–O distances, $1.99(1)$ – $2.06(1) \text{ \AA}$, are somewhat larger than those of the titanium analog [volume 672.5 \AA^3 , Ti–O distances $1.94(1)$ – $1.98(1) \text{ \AA}$].

The TGA measurements show simultaneous removal of the water and template molecules in one step starting at 380°C . According to X-ray powder diffraction, IR spectra, and TGA, calcination at 400°C for longer than 2 h leads to complete removal of the non-coordinated species, although some elemental carbon remains on the surface of the particles. Thermogravimetry shows that the structure collapses above 450°C (Fig. 4). The temperature dependence of the molar magnetic susceptibilities of the two compounds show Curie–Weiss behavior (Fig. 5). They were fitted with $\chi_m = C/(T - \theta) + \chi_0$, where χ_0 is a temperature-independent contribution to the paramagnetism. The accuracies of the two fits were better than 99.99% with the following parameters: $C = 1.45(1) \text{ emu K mol}^{-1}$, $\theta = -15.5(3) \text{ K}$, and $\chi_0 = 2(1) \times 10^{-4} \text{ emu mol}^{-1}$ for **1**, and $C = 0.892(1) \text{ emu K mol}^{-1}$, $\theta = -3.70(1) \text{ K}$, and $\chi_0 = 8.29(8) \times 10^{-4} \text{ emu mol}^{-1}$ for **2**. These Curie constants correspond to effective magnetic moments of 3.39 and $2.68 \mu_B$ for **1** and **2**, respectively.

4 Discussion

The first indication that compound **1** is isostructural with $\text{Ti}^{\text{III}}\text{Ti}^{\text{IV}}(\text{HPO}_4)_4 \cdot n\text{H}_2\text{O}$ came from its X-ray diffraction pattern. Later, this was confirmed by the similar lattice parameters and the identical body-centered tetragonal symmetry. This automatically suggests that the compound contains both V^{III} and V^{IV} . However, since, unlike titanium, such mixed

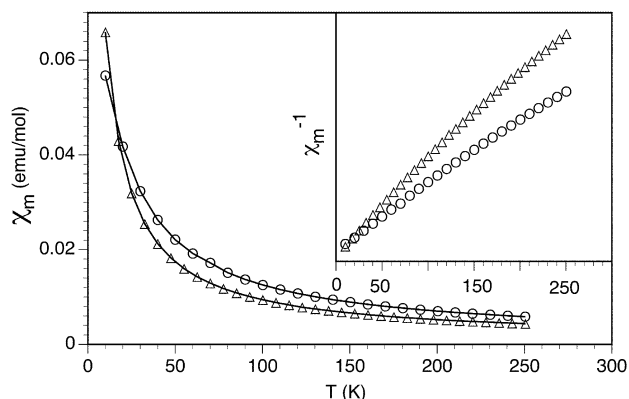


Fig. 5 Plot of the molar magnetic susceptibilities of **1** (\circ) and the product of its calcination at 400°C for 5 h, **2** (\triangle). The data were fitted with $\chi_m = C/(T - \theta) + \chi_0$ (the lines are the actual fits) and the parameters given in the text derived from the fits. The inset shows the temperature dependence of χ_m^{-1} for **1** and **2** (the slight deviations from linearity are caused by the small, but non-zero, χ_0 terms).

valence is not very common for vanadium, as mentioned in the Introduction, the valence states needed further study. Thus, high-resolution X-ray powder diffraction data were collected and the structure was refined. The refinement shows that the coordination octahedron around vanadium is quite regular. However, based on the fact that V^{IV} is often found in square-pyramidal or highly distorted octahedral coordination, some distortion was expected for the mixed $\text{V}^{\text{III/IV}}$ site. The observed regular octahedron would be consistent with a pure V^{III} site combined with eventual diprotonated ethylenediamine template, *i.e.* $\text{V}^{\text{III}}\text{V}^{\text{III}}(\text{HPO}_4)_4 \cdot n\text{H}_2\text{O}$. Furthermore, contrary to expectations, the overall V–O distances in **1** are longer than the corresponding distances in the titanium analog. This dilemma concerning the oxidation states of the vanadium atoms was resolved by the results of the magnetic measurements. They clearly show an effective magnetic moment of $3.39 \mu_B$ per formula unit. This is consistent with two magnetic centers of which one is d^2 and the other d^1 (V^{III} and V^{IV}). The spin-only moment for such a combination is calculated to be $3.32 \mu_B$, according to the formula $\mu = [n(n + 2) + m(m + 2)]^{1/2}$, where n and m are the numbers of unpaired electrons for each center, 1 and 2 in this case. For comparison, moments of 4.00 and $2.45 \mu_B$ are expected for two V^{III} and two V^{IV} centers, respectively. Thus, compound **1** is a mixed-valence $\text{V}^{\text{III}}/\text{V}^{\text{IV}}$ compound, just like the titanium analog, and the longer V–O distances are perhaps caused by the different coordination preferences of V^{IV} .

When calcined at 400°C for a few hours, compound **1** loses

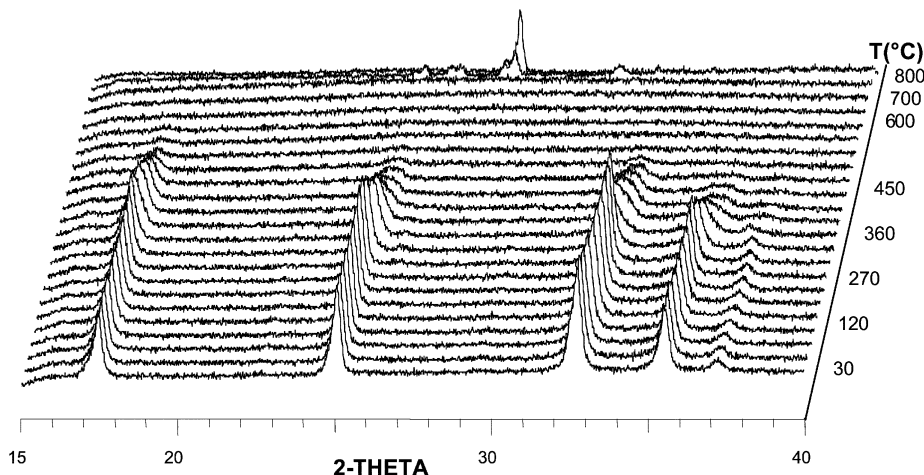


Fig. 4 Evolution of the X-ray powder diffraction pattern of **1** upon heating from 30 to 800°C (Co-K α radiation, $\lambda = 1.7903 \text{ \AA}$).

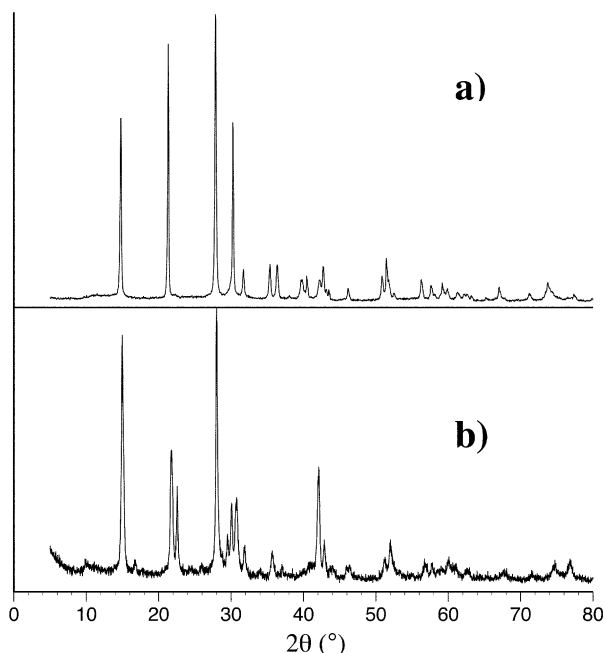


Fig. 6 Powder X-ray diffraction patterns of (a) $\text{V}^{\text{III}}\text{V}^{\text{IV}}(\text{HPO}_4)_4 \cdot n\text{H}_2\text{O}$ (**1**) and (b) its calcined form (heated at 400 °C for 2 h) $\text{V}^{\text{IV}}\text{V}^{\text{IV}}(\text{HPO}_4)_4$ (**2**). Both patterns are indexed in body-centered tetragonal symmetry. The cell of the calcined product is smaller and the peaks are shifted towards higher angles.

the template and water molecules (*ca.* 8 wt%), while the overall framework remains intact, and becomes compound **2**. The completion of this process was followed with IR spectroscopy by monitoring the characteristic peaks of ethylenediamine in the region 1500–1650 cm^{-1} . The crystallinity of compound **2**, however, was not suitable for X-ray studies and the data sets that were collected could not be refined satisfactorily. Nevertheless, it was possible to index the diffraction pattern and refine the lattice parameters. Apparently, compound **2** retains the body-centered tetragonal cell, but with a smaller volume, 664.7 \AA^3 compared to the 677.7 \AA^3 for compound **1**. As shown in Fig. 6, the diffraction peaks for compound **2** are shifted towards higher 2θ angles. In addition to this, some of the weak peaks in the pattern of **1** are quite intense in that of **2** and give the impression of lowered symmetry. However, the powder pattern of **2** was successfully indexed with the same $I4_1$ symmetry as compound **1**. One possible explanation for the compounds having the same symmetry but different peak intensities in their powder diffraction patterns is that in **2**, some atoms are shifted from their positions in **1**, but the overall framework is preserved as a whole. Such shifts are very likely to be associated with changes in the vanadium coordination upon changing its valence from mixed $\text{V}^{\text{III}}/\text{V}^{\text{IV}}$ to V^{IV} only, *i.e.* from regular octahedron to either square pyramid or extremely distorted octahedron. This is different from the titanium analog, which preserves both the symmetry and the overall peak intensity ratios upon heating because both Ti^{III} and Ti^{IV} prefer regular octahedral coordination. Despite the inability to collect data and refine the structure of compound **2**, it is clear from the magnetic measurements that vanadium is present only

as V^{IV} . Thus, the observed Curie–Weiss behavior of the magnetization and the measured magnetic moment of $2.68 \mu_{\text{B}}$ per formula unit with two vanadium atoms are consistent with this oxidation state. For comparison, the calculated spin-only moment for two d^1 centers is $2.45 \mu_{\text{B}}$. The oxidation of vanadium from V^{III} to V^{IV} compensates for the loss of one positive charge per formula unit associated with the removal of the monoprotonated ethylenediamine template in **1**. This keeps the charges balanced for the calcined compound **2** and is the reason for the preservation of the framework. The formula of **2** can be assigned, therefore, as $\text{V}^{\text{IV}}\text{V}^{\text{IV}}(\text{HPO}_4)_4$, in analogy with the calcined titanium compound.

Both calcined titanium and vanadium compounds, $\text{M}^{\text{IV}}\text{M}^{\text{IV}}(\text{HPO}_4)_4$, are potential materials for redox catalytic applications. However, the vanadium analog should be more interesting because of the non-zero number of d-electrons at the redox centers, the V^{IV} sites. The catalytic properties of the two compounds are being currently evaluated in various catalytic test reactions.

Acknowledgements

We thank the National Science Foundation (DMR-0139565), the Center for Molecularly Engineered Materials at Notre Dame, and the Centre National de la Recherche Scientifique (CNRS) for financial support.

References

- 1 I. W. C. E. Arends, R. A. Sheldon, M. Wallau and U. Schuchard, *Angew. Chem., Int. Ed. Engl.*, 1997, **36**, 1145 and references therein.
- 2 M. Hartmann and L. Kevan, *Chem. Rev.*, 1999, **99**, 635 and references therein.
- 3 I. W. C. E. Arends and R. A. Sheldon, *Appl. Catal., A*, 2002, **121**, 175 and references therein.
- 4 S. Ekambaram and S. C. Sevov, *Angew. Chem., Int. Ed.*, 1999, **38**, 372.
- 5 S. Ekambaram, C. Serre, G. Ferey and S. C. Sevov, *Chem. Mater.*, 2000, **12**, 444.
- 6 S. Ekambaram and S. C. Sevov, *Inorg. Chem.*, 2000, **39**, 2405.
- 7 E. Dumas, C. Debiemme-Chouy and S. C. Sevov, *J. Am. Chem. Soc.*, 2002, **124**, 908.
- 8 V. Soghomonian, R. C. Haushalter and J. Zubieta, *Chem. Mater.*, 1995, **7**, 1648.
- 9 R. C. Haushalter, Z. Wang, M. G. Thompson and J. Zubieta, *Inorg. Chem.*, 1993, **32**, 3700.
- 10 A. LeClaire, J. Chardon, M. M. Borel and B. Raneau, *J. Solid State Chem.*, 1994, **108**, 291.
- 11 J. W. Johnson, D. C. Johnson, H. E. King Jr., T. R. Halbert, J. F. Brody and D. P. Goshorn, *Inorg. Chem.*, 1988, **27**, 1646.
- 12 V. Soghomonian, Q. Chen, R. C. Haushalter and J. Zubieta, *Angew. Chem., Int. Ed. Engl.*, 1993, **32**, 610.
- 13 G. Bonavia, R. C. Haushalter and J. Zubieta, *J. Solid State Chem.*, 1996, **126**, 292.
- 14 Y. Zhang, A. Clearfield and R. C. Haushalter, *Chem. Mater.*, 1995, **7**, 1221.
- 15 P. Crespoa, A. Grandin, M. M. Borel, A. LeClaire and B. Raveau, *J. Solid State Chem.*, 1993, **105**, 307.
- 16 J. Rodriguez-Carjaval, in *Collected Abstracts of the Powder Diffraction Meeting of the XVth Congress of the IUCr, Toulouse, France, 1990*, International Union of Crystallography, 1990.
- 17 T. Roisnel and J. Rodriguez-Carvajal, *Mater. Sci. Forum*, 2001, **378–381**, 118.